REPORT DOCUMENTATION PAGE

Form Approved
OMB No. 0704-0188

1. REPORT DATE *(DD-MM-YYYY)*	2. REPORT TYPE	3. DATES COVERED *(From - To)*
13-05-2010	Journal Article	

4. TITLE AND SUBTITLE

Dinitrogen Difluoride Chemistry. Improved Synthesis of *cis*- and *trans*-N_2F_2, Synthesis and Characterization of $N_2F^+Sn_2F_9^-$, Ordered Crystal Structure of $N_2F^+Sb_2F_{11}^-$, High-Level Electronic Structure Calculations of *cis*-N_2F_2, *trans*-N_2F_2, $F_2N{=}N$, and N_2F^+, and Mechanism of the *trans-cis* Isomerization of N_2F_2 (Preprint)

5a. CONTRACT NUMBER

5b. GRANT NUMBER

5c. PROGRAM ELEMENT NUMBER

6. AUTHOR(S)
K. Christe, R. Haiges, & W. Wilson (USC); D. Dixon, D. Grant, & T.-H. Wang (University of Alabama); F. Tham (UC Riverside); A. Vij (AFRL/SE); V. Vij (ERC)

5d. PROJECT NUMBER

5e. TASK NUMBER

5f. WORK UNIT NUMBER
50260541

7. PERFORMING ORGANIZATION NAME(S) AND ADDRESS(ES)

Air Force Research Laboratory (AFMC)
AFRL/RZSP
10 E. Saturn Blvd.
Edwards AFB CA 93524-7680

8. PERFORMING ORGANIZATION REPORT NUMBER

AFRL-RZ-ED-JA-2010-254

9. SPONSORING / MONITORING AGENCY NAME(S) AND ADDRESS(ES)

Air Force Research Laboratory (AFMC)
AFRL/RZS
5 Pollux Drive
Edwards AFB CA 93524-70448

10. SPONSOR/MONITOR'S ACRONYM(S)

11. SPONSOR/MONITOR'S NUMBER(S)
AFRL-RZ-ED-JA-2010-254

12. DISTRIBUTION / AVAILABILITY STATEMENT

Approved for public release; distribution unlimited (PA #10257).

13. SUPPLEMENTARY NOTES
For publication in Inorganic Chemistry.

14. ABSTRACT
N2F+ salts are important precursors in the synthesis of N5+ compounds, and better methods are reported for their larger scale production. A new, marginally stable N2F+ salt, N2F+Sn2F9-, was prepared and characterized. An ordered crystal structure was obtained for N2F+Sb2F11-, resulting in the first observation of individual N≡N and N-F bond distances for N2F+ in the solid phase. The observed N≡N and N-F bond distances of 1.089(9) and 1.257(8) Å, respectively, are among the shortest experimentally observed N-N and N-F bonds. High-level electronic structure calculations at the CCSD(T) level with correlation-consistent basis sets extrapolated to the complete basis limit show that cis-N2F2 is more stable than trans-N2F2 by 1.4 kcal/mol at 298 K. The calculations also demonstrate that the lowest uncatalyzed pathway for the trans-cis isomerization of N2F2 has a barrier of 60 kcal/mol and involves rotation about the N=N double bond. This barrier is substantially higher than the energy required for the dissociation of N2F2 to N2 and 2 F. Therefore, some of the N2F2 dissociates before undergoing an uncatalyzed isomerization, with some of the dissociation products probably catalyzing the isomerization. Furthermore, it is shown that the trans-cis isomerization of N2F2 is catalyzed by strong Lewis acids, involves a planar transition state of symmetry Cs, and yields a 9:1 equilibrium mixture of cis-N2F2 and trans-N2F2. Explanations are given for the increased reactivity of cis-N2F2 with Lewis acids and the exclusive formation of cis-N2F2 in the reaction of N2F+ with F-. The geometry and vibrational frequencies of the F2N=N isomer have also been calculated and imply strong contributions from ionic N2F+ F- resonance structures, similar to those in F3NO and FNO.

15. SUBJECT TERMS

16. SECURITY CLASSIFICATION OF:			17. LIMITATION OF ABSTRACT	18. NUMBER OF PAGES	19a. NAME OF RESPONSIBLE PERSON
					Mr. Wayne Kalliomaa
a. REPORT	b. ABSTRACT	c. THIS PAGE			19b. TELEPHONE NUMBER *(include area code)*
Unclassified	**Unclassified**	**Unclassified**	SAR	38	N/A

Dinitrogen Difluoride Chemistry. Improved Syntheses of *cis*– and *trans*–N_2F_2, Synthesis and Characterization of $N_2F^+Sn_2F_9^-$, Ordered Crystal Structure of $N_2F^+Sb_2F_{11}^-$, High-Level Electronic Structure Calculations of *cis*-N_2F_2, *trans*-N_2F_2, $F_2N{=}N$, and N_2F^+, and Mechanism of the *trans-cis* Isomerization of N_2F_2[†] (Preprint)

Karl O. Christe,[*§] David A. Dixon,[#] Daniel J. Grant,[#] Ralf Haiges,[§] Fook S. Tham,[⊥] Ashwani Vij,[‡] Vandana Vij,[‡] Tsang-Hsiu Wang,[#] and William W. Wilson[§]

[§] Loker Hydrocarbon Research Institute and Department of Chemistry, University of Southern California, Los Angeles, CA 90089,USA, [#] Department of Chemistry, University of Alabama, Tuscaloosa, AL 35487-0336, USA, [⊥] Department of Chemistry, University of California, Riverside, CA 92521, and [‡]Space and Missile Propulsion Division, Air Force Research Laboratory (AFRL/RZS), Edwards Air Force Base, CA 93524, USA

[†]This paper is dedicated to the memory of Ira B. Goldberg

*To whom correspondence should be addressed. E-mail: kchriste@usc.edu

Abstract

N_2F^+ salts are important precursors in the synthesis of N_5^+ compounds, and better methods are reported for their larger scale production. A new, marginally stable N_2F^+ salt, $N_2F^+Sn_2F_9^-$, was prepared and characterized. An ordered crystal structure was obtained for $N_2F^+Sb_2F_{11}^-$, resulting in the first observation of individual N≡N and N-F bond distances for N_2F^+ in the solid phase. The observed N≡N and N-F bond distances of 1.089(9) and 1.257(8) Å, respectively, are among the shortest experimentally observed N-N and N-F bonds. High-level electronic structure calculations at the CCSD(T) level with correlation-consistent basis sets extrapolated to the complete basis limit show that *cis*-N_2F_2 is more stable than *trans*-N_2F_2 by 1.4 kcal/mol at 298 K.

The calculations also demonstrate that the lowest uncatalyzed pathway for the *trans*-*cis* isomerization of N_2F_2 has a barrier of 60 kcal/mol and involves rotation about the N=N double bond. This barrier is substantially higher than the energy required for the dissociation of N_2F_2 to N_2 and 2 F. Therefore, some of the N_2F_2 dissociates before undergoing an uncatalyzed isomerization, with some of the dissociation products probably catalyzing the isomerization. Furthermore, it is shown that the *trans*-*cis* isomerization of N_2F_2 is catalyzed by strong Lewis acids, involves a planar transition state of symmetry C_s, and yields a 9:1 equilibrium mixture of *cis*-N_2F_2 and *trans*-N_2F_2. Explanations are given for the increased reactivity of *cis*-N_2F_2 with Lewis acids and the exclusive formation of *cis*-N_2F_2 in the reaction of N_2F^+ with F^-. The geometry and vibrational frequencies of the $F_2N{=}N$ isomer have also been calculated and imply strong contributions from ionic N_2F^+ F^- resonance structures, similar to those in F_3NO and FNO.

Introduction

Polynitrogen compounds possess high energy and hold great potential as propellants and explosives.[1,2] In 1999, the isolation of an exciting new polynitrogen compound, $N_5^+AsF_6^-$, was reported.[1] The synthesis of $N_5^+AsF_6^-$ [1] and other N_5^+ salts[2] was achieved by reacting N_2F^+ salts with HN_3 in a suitable solvent. The following 5-step process, originally used for generating the required N_2F^+ salt (Scheme 1), was expensive, time consuming and sometimes gave undesirable by-products.

$$C_x + AsF_5 \rightarrow C_x{\cdot}AsF_5 \qquad (x = 10\text{-}12) \qquad (1)$$

$$2\ C_x{\cdot}AsF_5 + N_2F_4 \rightarrow 2\ C_x^+AsF_6^- + \textit{trans}\text{-}N_2F_2 \qquad (2)$$

$$\textit{trans}\text{-}N_2F_2 + AsF_5 \rightarrow N_2F^+AsF_6^- \qquad (3)$$

$$N_2F^+AsF_6^- + NaF \rightarrow NaAsF_6 + \textit{cis}\text{-}N_2F_2 \qquad (4)$$

$$\textit{cis}\text{-}N_2F_2 + MF_5 \rightarrow N_2F^+MF_6^- \qquad (5)$$

Scheme 1

The synthesis of N_2F^+ salts required the commercially unavailable N_2F_2. The latter can exist as both a *cis*– and a *trans*–isomer, but only the *cis*–isomer reacts readily at ambient or sub-ambient temperatures with strong Lewis acids to form the desired N_2F^+ salts. Both isomers are planar, with C_{2v} symmetry for the *cis*– and C_{2h} symmetry for the *trans*–isomer. The *cis*–isomer has been reported to be thermodynamically slightly more stable than the *trans*–isomer.[3,4] While most preparative methods for N_2F_2 result in mixtures of both isomers,[3] its most convenient synthesis involving the reduction of N_2F_4 with graphite/AsF_5 intercalates,[5] produces only the less reactive *trans*–isomer which must then be converted into the *cis*–isomer. Although *trans–cis* isomerization has been reported[6] to occur above 225 °C in a copper flow tube, the uncatalyzed

reaction has a very high activation energy barrier with calculated values[4] ranging from 65 to 85 kcal mol^{-1}. However at these temperatures, the thermal decomposition of N_2F_2 to NF_3, N_2 and F_2 proceeds quite readily. Therefore, the high temperature gas phase isomerization must compete with the decomposition reaction which might result in autocatalysis and renders the isomerization reaction difficult to control. A reported experimental barrier[7] of only 32 kcal mol^{-1} for the gas phase isomerization reaction is suspect[8] and needs verification. Isomerizations at temperatures below 225 °C involve long induction periods of weeks or months consistent with the calculated high barriers and the possible need for creating first catalytically active metal fluoride surfaces by the reaction of some fluorine decomposition product with metal components. Therefore, finding convenient and reproducible isomerization conditions was important for scale-up reactions. In the past,[1,9] this problem had been overcome by reacting *trans*–N_2F_2 with the strong Lewis acid AsF_5 under carefully controlled conditions, 75 °C and elevated pressure, to give $N_2F^+AsF_6^-$. Subsequent displacement reactions of the resulting $N_2F^+AsF_6^-$ with a strong Lewis base, such as FNO or alkali metal fluorides in HF solution, resulted in the exclusive formation of *cis*–N_2F_2, thus providing a high-yield but cumbersome method for the synthesis of pure *cis*–N_2F_2, which then could be used for the synthesis of N_2F^+ salts other than AsF_6^-.

Further drawbacks of the previous process[1] were the use of expensive Highly Oriented Pyrolytic Graphite (HOPG) for preparing the AsF_5 intercalate and the need for long reaction times, stoichiometric amounts of AsF_5 and an extra step, the displacement reaction. In this paper experimental solutions are presented which mitigate these problems. Using high-level quantum chemical calculations, a better understanding of the underlying chemistry was also gained and some of the questions concerning the mechanism and thermodynamics of the N_2F_2 *trans–cis*

isomerization[9] were answered. With the crystal structure of $N_2F^+Sb_2F_{11}^-$, the first ordered structure of an N_2F^+ salt was determined and the synthesis of the new N_2F^+ salt, $N_2F^+Sn_2F_9^-$, is communicated. In addition, a theoretical study of the $F_2N{=}N$ isomer was carried out, resulting in the prediction of an unusual structure with highly ionic N-F bonds, similar to those found in F_3NO[10] and FNO.[11,12]

Experimental Section

Caution! Some of the compounds used in this study are strong oxidizers and anhydrous HF is corrosive and can cause severe burns on contact with skin. Recommended safety precautions include the wearing of face shields, leather gloves and protective leather clothing.

Materials and Apparatus: Arsenic pentafluoride (Advanced Research Chemicals) and N_2F_4 (Air Products) were purified by fractional condensation prior to use. Fluorine (Allied Chemical) and antimony pentafluoride (Ozark Mahoning) were used as received. Powdered natural graphite flakes (Asbury Graphite Mills, No. 3243 50-60 μ) were treated with 360 torr of fluorine gas to remove traces of moisture and reactive impurities before their intercalation with AsF_5. Hydrogen fluoride (Matheson Co.) was dried over BiF_5 as described earlier.[13] Due to the corrosive and hazardous nature of the compounds used during this work, a stainless steel Teflon-FEP vacuum line, fitted with Hoke valves, was used.[14] The vacuum line and all reaction vessels were passivated with ClF_3 prior to use. Pressures were measured with a Heise-Bourdon tube-type gauge (0-1500 mm ± 0.1%). All non-volatile materials were handled in the inert atmosphere of a glove box.

Infrared spectra were recorded on a Mattson Galaxy FTIR spectrometer. The Raman spectra were measured either on a Cary Model 83GT spectrometer using the 488-nm line of an

Ar-ion laser or on a Bruker Equinox 55 spectrometer using the 1064 nm line of a Nd-Yag laser. The infrared spectra of gaseous samples were taken using a Monel IR cell equipped with a stainless steel valve and AgCl windows. The spectra of solid samples were recorded as powders pressed between AgCl or AgBr windows.

The single crystal X-ray diffraction data were collected on a Bruker 3-circle platform diffractometer equipped with a SMART CCD (charge coupled device) detector with the χ-axis fixed at 54.74° and using MoK_α radiation (λ = 0.71073 Å) from a fine-focus tube. This diffractometer was equipped with an LT-3 apparatus for low-temperature data collection using controlled liquid nitrogen boil off. Single crystals were selected in a glovebox, equipped with a CCD camera mounted microscope, and immersed in a culture slide's cavity containing PFPE (perfluoropolyether) oil. The culture slide was then taken out of the glovebox, and a suitable crystal was scooped out with a magnetic Cryoloop and mounted in a cold nitrogen stream on the magnetic goniometer head. Cell constants were determined from 90 30-sec frames. A complete hemisphere of data was scanned on omega (0.3°) with a run time of 30-sec per frame at a detector resolution of 512 x 512 pixels using the SMART software.[15] A total of 1271 frames were collected in three sets. A final set of 50 frames, identical to the first 50 frames, was also collected to determine if any crystal decay had occurred. The frames were then processed on a PC by using the SAINT software[16] to give the hkl file corrected for Lp/decay. The absorption correction was performed using the SADABS[17] program. The structures were solved by the direct method using the SHELX-90[18] program and refined by the least squares method on F2, SHELXL-97,[19] incorporated in SHELXTL Suite 5.10 for Windows NT.[20]All atoms were refined anisotropically. For the anisotropic displacement parameters, the U(eq) is defined as one third of the trace of the orthogonalized U_{ij} tensor.

Intercalation of Graphite with AsF_5. Natural graphite flakes (120 g, 1 mol based on C_{10}) were loaded into a prepassivated 1 L Monel cylinder, which was then attached to a steel vacuum line and evacuated. Teflon filters were used to prevent any graphite powder from being blown into the line. About 25 mmol of fluorine gas was slowly bled into the evacuated cylinder. After keeping the cylinder for 12 h at room temperature, unreacted fluorine was pumped off and passed through a –196 °C trap followed by a soda-lime scrubber. The volatiles trapped at –196 °C, consisted mainly of CO_2, CF_4, SiF_4, HF, and a trace of C_2F_6. Then, AsF_5 (173 g, 1.02 mol) was slowly bled at room temperature into the reactor, and a rapid pressure drop indicated the onset of intercalation. The total AsF_5 addition took about 2 h, after which the AsF_5 uptake became negligible. At this point, the cylinder was cooled to –196 °C and the remaining AsF_5 was condensed in. The cylinder was warmed to room temperature for ~72 h after which time the volatiles were pumped off through a –196 °C trap. The contents of this trap consisted of small amounts of AsF_3, CF_4 and SiF_4 and showed only traces of AsF_5. The graphite showed a weight gain of 141g (0.83 mol of AsF_5) indicative of a first stage intercalate having the approximate composition $C_{12}AsF_5$. This intercalate was subsequently used to reduce the N_2F_4 to N_2F_2.

In a separate experiment, the cylinder was heated to 45 °C after condensing the AsF_5 onto the graphite. This resulted in a lower weight uptake and the generation of large amounts of AsF_3 along with other decomposition products. Therefore, heating must be avoided when carrying out the intercalation reaction.

Reduction of N_2F_4 with the Graphite Intercalate. This reaction was carried out as described by Selig,[5] but the reaction time was reduced to ~38 h as opposed to ~5 days. In a typical experiment, 200 mmol of N_2F_4 was condensed at –196 °C into an evacuated 300 mL stainless steel reactor containing 138 mmol of $C_{12}AsF_5$. The cylinder was allowed to warm

slowly to room temperature and kept at this temperature for 38 h. Noncondensible material, mainly nitrogen gas, was removed by evacuating the reactor at –196 °C. The room temperature volatiles were fractionated through traps held at –156 and –196 °C. The –156 °C trap contained *trans*–N_2F_2 (194.5 mmol, ~97% yield based on N_2F_4), while the –196 °C trap contained some NF_3 and CF_4.

Isomerization Reactions of *trans*–N_2F_2. A reaction between *trans*–N_2F_2 (103 mmol) and SbF_5 (19.42 mmol) was carried out in a 100 mL Monel cylinder for 6 days at room temperature. The cylinder was then cooled to –196 °C and checked for any non-condensable material. None was detected. It was then kept in a –64 °C bath, and the volatiles were pumped through traps held at –156 and –196 °C. Nothing was trapped at –156 °C, and the –196 °C trap contained mainly *cis*–N_2F_2 (~75 mmol) and smaller amounts of *trans*–N_2F_2, NF_3 and CF_4. In the reactor, a white solid remained consisting of $N_2F^+Sb_2F_{11}^-$ (~3.5g).

In another experiment, a 30 mL passivated 316-stainless steel cylinder was loaded in the glove box with AlF_3 (0.7mmol) and attached to the vacuum line. The cylinder was evacuated and treated with 800 torr of F_2 for 16 h at room temperature. After removal of the F_2, the cylinder was cooled to –196 °C, evacuated, and *trans*–N_2F_2 (12.1 mmol) was condensed in. The reactor was allowed to warm to room temperature and then heated in an oil bath to 55 °C for 16 h, cooled to room temperature. It was checked for any non-condensable material at –196 °C, but none was detected. The room-temperature volatiles (12.0 mmol) were trapped at –196 °C and consisted of *cis*–N_2F_2 (90 %), *trans*–N_2F_2 (10 %) and a trace of NF_3.

When this experiment was repeated under identical conditions in a prepassivated 316-stainless steel reactor but in the absence of AlF_3, identical results (90 % *cis*– and 10 % *trans*–N_2F_2) were obtained.

However, when the experiment was scaled up to 40 mmol of *trans*–N_2F_2 in the same size 30 mL prepassivated 316-stainless steel cylinder, a strongly exothermic reaction occurred upon insertion into the oil bath at 55 °C, resulting in a sharp temperature rise and complete decomposition of the *trans*–N_2F_2 to NF_3, N_2 and F_2.

In a separate experiment, a 10 mL Teflon-FEP reactor, containing 30 mg of AlF_3, was loaded with *trans*–N_2F_2 (0.77 mmol) and heated to 55 °C for 16 h, resulting in a 90 % conversion of *trans*–N_2F_2 to *cis*–N_2F_2.

In a similar experiment in a Teflon reactor but in the absence of AlF_3, no isomerization of *trans*–N_2F_2 was observed.

Preparation of $N_2F^+SbF_6^-$ and $N_2F^+Sb_2F_{11}^-$. In order to obtain well-defined stoichiometries, exact amounts of SbF_5 and *cis*–N_2F_2 were combined in anhydrous HF solution. For this purpose, a prepassivated Teflon ampule, equipped with a stainless steel Hoke valve and a Teflon coated magnetic stirring bar, was loaded in the glove box with SbF_5 (20.3 mmol), attached to the vacuum line and evacuated at –196 °C. Anhydrous HF (~2 mL) was condensed into the ampule, and the reaction mixture was allowed to warm to ambient temperature to dissolve the SbF_5. The ampule was cooled to –196 °C, and a slight excess of *cis*–N_2F_2 (~22 mmol) was added. The ampule was allowed to warm slowly toward room temperature and then stirred vigorously for about 10 min. The volatiles were pumped off at –64 °C for 2 h until a constant weight was attained, leaving behind a white free flowing powder. The observed weight gain (5.71 g) corresponded to the formation of 20.2 mmol of $N_2F^+SbF_6^-$ (99.7% yield based on SbF_5).

The $N_2F^+Sb_2F_{11}^-$ salt was prepared in a similar manner by reacting 3.1 mmol of SbF_5 with 3.1 mmol of $N_2F^+SbF_6^-$ in ~2 mL of HF. $N_2F^+Sb_2F_{11}^-$ was obtained as a white flaky solid in

quantitative yield. The infrared and Raman spectra of these compounds agreed well with those reported in literature.[9,21-25]

Synthesis of $N_2F^+Sn_2F_9^-$. When anhydrous HF suspensions of SnF_4 were treated for several days at ambient temperature in either Teflon-FEP ampules or 316-stainless steel cylinders with a two- to four-fold molar excess of *cis*–N_2F_2, white solid residues were obtained upon removal of the volatile products. Based on the observed material balances, the combining ratios of SnF_4 : *cis*–N_2F_2 were always very close to 2 : 1. The Raman and infrared spectra of these solids showed the presence of bands due to N_2F^+ cations[9,21-25] and tin fluoride anions.[26-28] Therefore, the empirical composition of these solids is best described as $N_2F^+Sn_2F_9^-$. In one instance, a solid was obtained with a composition closer to 1:1, the vibrational spectra of which showed the presence of trapped *cis*–N_2F_2,[29] indicating that salts richer in N_2F^+, such as $N_2F^+SnF_5^-$, are thermally unstable at room temperature and decompose with the evolution of *cis*-N_2F_2.

Crystal Structure Determination of $N_2F^+SbF_6^-$. Single crystals of $N_2F^+SbF_6^-$ were grown from HF solutions at –45 °C in a Teflon-FEP ampule. The solvent was slowly removed by distillation in a static vacuum into a –78 °C trap. Suitable crystals were selected in the drybox and mounted as described in the Experimental Section. The diffraction data indicated no crystal decay during the data collection, but the nylon loop was charred when the mounted crystal was allowed to warm to room temperature. The intensity statistics and E-values did not provide an unambiguous choice of space groups in the orthorhombic crystal system. Systematic absences, *i.e.*, absence of $h+k$ = odd reflections, however, clearly indicated a *C*-centered lattice. The structure could be solved in both centrosymmetric (*Cmmm*) and non-centrosymmetric space groups (*C*222 and *Amm*2). The *Cmmm* and *C*222 space groups placed the central nitrogen atom,

bonded to one other atom – nitrogen or fluorine, of the N_2F^+ cation on a mirror plane, thereby generating disorder in the N-N-F bonds. The structure was refined with nitrogen and fluorine atoms on the same sites with equal occupancy factors. This model failed to give the individual N-N and N-F bond distances and, therefore, provided information only on the $r_{N\equiv N} + r_{N-F}$ distances. Both these space groups refine the structure to the same *R*-value of 3.9% and similar structural parameters were obtained. The final choice of *Cmmm* to be the correct space group was made on the basis that this space group has higher symmetry and only half of the parameters need to be refined. An alternate choice of the *Amm2* space group was rejected although it allowed the determination of individual N-N and N-F bonds, because the atoms did not have good thermal values and the *R*-value was considerably higher.

Crystal Structure Determination of $N_2F^+Sb_2F_{11}^-$. The $N_2F^+Sb_2F_{11}^-$ crystals obtained from the reaction of *trans*–N_2F_2 with SbF_5 at room temperature were used for this diffraction study. A suitable single crystal was mounted using a Cryoloop as described above. The intensity statistics, i.e., E^2-1 values, indicated a centrosymmetric space group for $N_2F^+Sb_2F_{11}^-$. Furthermore, the absence of 0 *k* 0 (*k* = odd) and *h*0*l* reflections (*h*+*l* = odd) showed the presence of a 2_1 screw axis and an *n*-glide plane parallel and perpendicular to the *b*-axis, respectively. The space group was thus unambiguously assigned as $P2_1/n$.

Computational Methods. The computational approach developed at The University of Alabama and Washington State University for the prediction of accurate molecular thermochemistry was used to predict the heats of formation and important energetic features of these compounds.[30-32] The approach is based on calculating the total atomization energy of a molecule and using this value with known heats of formation of the atoms to calculate the heat of formation at 0 K. The approach starts with coupled cluster theory with single and double

excitations and includes a perturbative triples correction (CCSD(T)),[33-35] combined with the correlation-consistent basis sets[36] extrapolated to the complete basis set (CBS) limit to treat the correlation energy of the valence electrons. This is followed by a number of smaller additive corrections including core-valence interactions and relativistic effects, both scalar and spin-orbit. The zero point energy can be obtained from experiment, theory, or a combination of the two. Corrections to 298 K can then be calculated by using standard thermodynamic and statistical mechanics expressions in the rigid rotor-harmonic oscillator approximation[37] and appropriate corrections for the heat of formation of the atoms.[38]

The standard aug-cc-pV*n*Z basis sets were used for N and F and abbreviated as aV*n*Z. Only the spherical component subset (e.g., 5-term *d* functions, 7-term *f* functions, etc.) of the Cartesian polarization functions were used. All CCSD(T) calculations were performed with the MOLPRO-2002 program system[39] on an SGI Altix computer, the Cray XD-1, the dense memory Linux cluster at the Alabama Supercomputer Center, or the Dell Linux cluster at The University of Alabama. For the open shell atomic calculations, the restricted method for the starting Hartree-Fock wavefunction was used and then the spin restriction in the coupled cluster portion of the calculation was relaxed. This method is conventionally labeled R/UCCSD(T).[40-42]

The geometries were optimized at the CCSD(T) level with the aVDZ and aVTZ basis sets except for N_2F where only the aVDZ geometry was obtained. The aVTZ geometries were then used in single point CCSD(T)/aVQZ calculations. The zero point energies (ΔE_{ZPE}) were calculated at the CCSD(T)/aVTZ level without scaling. For the CBS estimates, a mixed exponential/Gaussian function of the form[43]

$$E(n) = E_{CBS} + Be^{-(n-1)} + Ce^{-(n-1)^2} \qquad (6)$$

was used, where n = 2 (aVDZ), 3 (aVTZ), and 4 (aVQZ). Core-valence (CV) calculations were carried out at the CCSD(T) level with the weighted CV basis set cc-pwCVTZ.[44] The atomic spin-orbit corrections are $\Delta E_{SO}(O) = 0.22$, $\Delta E_{SO}(F) = 0.39$, and $\Delta E_{SO}(F^+) = 0.48$ kcal/mol, respectively, taken from the tables of Moore.[45] ΔE_{SR} was evaluated by using expectation values for the two dominant terms in the Breit-Pauli Hamiltonian, the so-called mass-velocity and one-electron Darwin (MVD) corrections from configuration interaction singles and doubles (CISD) calculations[46] with the a VTZ basis set at the appropriate optimized geometry. By combining the computed ΣD_0 values, given by the following expression,

$$\Sigma D_0 = \Delta E_{elec}(CBS) - \Delta E_{ZPE} + \Delta E_{CV} + \Delta E_{SR} + \Delta E_{SO} \quad (7)$$

with the known heats of formation at 0 K for the elements, the $\Delta H_{f,0K}$ values can be derived. The heats of formation of N and F are $\Delta H_{f,0K}(N) = 112.53$ kcal/mol and $\Delta H_{f,0K}(F) = 18.47$ kcal/mol.[47] Heats of formation at 298 K were obtained by following the procedures outlined by Curtiss et al.[38]

Results and Discussion

Preparation of the Graphite·AsF_5 Intercalate. The first step in the generation of N_2F^+ salts is the formation of a first stage intercalate of AsF_5 in graphite (Eq. 1). If HOPG (Highly Oriented Pyrolytic Graphite) is used, the intercalation is sluggish and requires several weeks to go to completion. Not only is HOPG very expensive, it is also difficult to grind. Replacing the HOPG graphite with finely powdered natural flake graphite (particle size of 50-60 μ), which is commercially available for about one dollar per pound, proved to be a highly efficient and economical method for preparing the required intercalate. In all the intercalation experiments performed during this work, the graphite powder was pretreated with small amounts of ambient

pressure F_2 gas to remove impurities and traces of moisture. The major volatile products observed during this treatment were CF_4 and SiF_4. In different runs of the intercalation reaction, carried out at room temperature with reaction times of 2-3 days, the composition of the first-stage intercalate based on AsF_5 uptake corresponded to C_xAsF_5 (x = 10.4-12.0). Furthermore, it was found that mild warming of the reaction cylinder to ~40 ºC accelerated the intercalation, but also resulted in the formation of significant amounts of CF_4 and AsF_3 due to the oxidation of the graphite by AsF_5. Therefore, heating of the cylinder to accelerate the intercalation rate should be avoided. As reported earlier, AsF_3 does not form a stable intercalate with graphite.[5]

Synthesis of *trans*–N_2F_2. Our method for the preparation of *trans*-N_2F_2 was based on the work of Münch and Selig,[5] and involved the reduction of N_2F_4 with the graphite/AsF_5 intercalate (Eq. 2). Without careful temperature control, varying amounts of N_2, F_2 and NF_3 were obtained with traces of SiF_4 and CF_4 as by-products. However, addition of the N_2F_4 at –196 ºC, followed by slow and controlled warm up and use of the small particle size, natural flake graphite intercalate, resulted in a fast and quantitative reduction of the N_2F_4 to *trans*–N_2F_2 without formation of NF_3, N_2 and F_2. The quantitative formation of *trans*-N_2F_2 also eliminated its difficult separation from unreacted N_2F_4. No *cis*–N_2F_2 was observed in all of these reactions.

Münch and Selig reported[5] that the reaction of first stage graphite/AsF_5 intercalate with N_2F_4 was complete after one mole of N_2F_4 was converted per mole of intercalated AsF_5. We examined the stoichiometry of this reaction by adding the N_2F_4 in increments to the first stage intercalate and analyzing the products after each N_2F_4 addition. Contrary to the report by Münch and Selig,[5] we found that 1 mol of intercalate was able to quantitatively reduce somewhat more than 1.5 mol of N_2F_4 to *trans*–N_2F_2. This demonstrates that equation (2) is a poor description of this reaction and that the graphite structure is also being fluorinated (Eq. 8).

$$2\ C_{12}{\cdot}AsF_5\ +\ 3\ N_2F_4\ \rightarrow\ 2\ C_{12}F_2{}^{+}AsF_6{}^{-}\ +\ 3\ \textit{trans}{-}N_2F_2 \qquad (8)$$

Reaction of N_2F_2 with Lewis Acids and its *trans–cis* Isomerization. In the previous study,[9] excess *trans*–N_2F_2 was reacted with AsF_5 at 70 °C for 3 days to give yields of $N_2F^+AsF_6^-$ of about 80% (Eq. 3). In this study, it was found that by cutting the reaction time in half, the yield of $N_2F^+AsF_6^-$ could be increased to >99%, based on the amounts of AsF_5 used, and the decomposition of N_2F_2 to NF_3, N_2 and F_2 was suppressed. By adding the required amount of NaF to the cylinder containing the $N_2F^+AsF_6^-$, condensing in HF and shaking it vigorously at room temperature, quantitative yields of *cis*–N_2F_2 were obtained (Eq. 4), which can then be converted readily to other N_2F^+ salts, such as $N_2F^+SbF_6^-$, by reaction with the corresponding Lewis acid (Eq. 5).

When either $N_2F^+Sb_2F_{11}^-$ is the desired product or the loss of some N_2F_2 in the form of $N_2F^+Sb_2F_{11}^-$ can be tolerated, steps (3) and (4) can be greatly simplified by replacing the stoichiometric amount of AsF_5 required for (3) by catalytic amounts of SbF_5, thus avoiding the use of large amounts of expensive AsF_5 and eliminating the need for heating and for the displacement step (4). Thus, when *trans*–N_2F_2 was reacted for 6 days at room temperature with catalytic amounts of SbF_5, the 9 : 1 *cis–trans*–N_2F_2 equilibrium was established, while the catalytic amount of SbF_5 was converted to $N_2F^+Sb_2F_{11}^-$ (Eq. 9). The $N_2F^+Sb_2F_{11}^-$ was characterized by vibrational spectroscopy and its crystal structure (see below).

$$\underset{\text{excess}}{\textit{trans}{-}N_2F_2}\ +\ 2\ SbF_5\ \xrightarrow[\text{rt}]{}\ N_2F^+Sb_2F_{11}^-\ +\ \textit{cis}{-}N_2F_2 \qquad (9)$$

The most effective catalysts, however, were found to be either 10-20 mol% of commercial AlF_3, which had been pretreated with elemental F_2 gas at 60 °C, or the surfaces of 316-stainless steel cylinders, which had been passivated with strong fluorinating agents, such as

F_2 or ClF_3. Running these isomerization reactions at 55 °C for 15 h, the limiting thermodynamic *cis–trans* equilibrium[3,48] of 9 : 1 can successfully be reached. Examination of the used AlF_3 catalyst by Raman spectroscopy at room temperature showed no evidence for the presence of N_2F^+ salts or retention of N_2F_2 by AlF_3. Furthermore, the catalyst was reusable and not consumed. We have also demonstrated that heating alone in the absence of a catalyst, i.e., using an all Teflon reactor under the same conditions, did not result in isomerization.

Since N_2F_2 is thermodynamically unstable with respect to its decomposition products NF_3, N_2 and F_2,[3] and stainless steel is a relatively poor thermal conductor, heating of steel cylinders, overloaded with N_2F_2, can lead to exothermic, uncontrolled thermal decomposition of the N_2F_2. Such an event was observed by us when a 30 mL prepassivated stainless steel reactor, loaded with 40 mmol of *trans*–N_2F_2, was immersed into a 55 °C oil bath, resulting in a run-away exothermic decomposition reaction of all the N_2F_2 present. In a second case, a similarly overloaded reactor, but this time in the presence of catalytic amounts of SbF_5, also underwent N_2F_2 decomposition. The generated heat and pressure were sufficient to effect the reaction of SbF_5 with the NF_3 and F_2 decomposition products to yield $NF_4^+Sb_3F_{16}^-$ according to (10).[49]

$$3\ SbF_5 + NF_3 + F_2 \rightarrow NF_4^+Sb_3F_{16}^- \qquad (10)$$

It should be noted that the catalytic effect of prepassivated steel on the isomerization had already been mentioned more than 40 years ago,[48,50] but has been widely ignored in subsequent work.

Structural Investigations of $N_2F^+SbF_6^-$ and $N_2F^+Sb_2F_{11}^-$. The N_2F^+ cation has been the subject of various spectroscopic, structural and theoretical investigations.[3,9,21-24,51-57] The most interesting features are the unusually short N-N and N-F bond lengths of 1.1034(5) and 1.2461(10) Å, respectively, observed by Botschwina et al. for the free gaseous ion using millimeter-wave spectroscopy.[52] The shortest experimentally observed N-N bond distance is

1.09277(9) Å in N_2H^+.[58] Christe et al. have previously determined the crystal structure of $N_2F^+AsF_6^-$.[9] The compound crystallized in the centrosymmetric space group *C*2*m* where the N≡N and N-F bonds were disordered, and it was not possible to measure the bond lengths of each bond individually. The same disorder problem affects the crystal structure of $N_2F^+SbF_6^-$ in the present study, and only the sum of the N-N and N-F bond distances (2.340(9) Å) can be determined. Details on the disordered $N_2F^+SbF_6^-$ structure are given in the Supplementary Material.

The crystal structure of $N_2F^+Sb_2F_{11}^-$ (Tables 1,2 and S4) is ordered and allows the determination of the individual N-N and N-F bond lengths. This structure can be considered a true representation of the N_2F^+ cation in the solid-state and the linearity of the N-N-F bond is not automatically generated by symmetry as in the case of $N_2F^+MF_6^-$ (M = As or Sb) salts. The structure (Fig. 1) was solved in the $P2_1/n$ space group and all of the atoms showed excellent thermal behavior. A final *R* value of 3.76% was obtained with no appreciable residual electron density left over, which would indicate some disorder. The sum of the N-N and N-F bond distances of 2.346(9) Å (Table 3) is in excellent agreement with the observed spectroscopic gas phase value of 2.3495 Å.[52] In $N_2F^+Sb_2F_{11}^-$, the N-F distance of 1.257(8) Å is somewhat longer and the N-N distance of 1.089(9) Å is slightly shorter than those (1.2461 and 1.1034 Å, respectively,) of gaseous N_2F^+.[52] The N≡N distance in $N_2F^+Sb_2F_{11}^-$ can, therefore, be considered to be among the shortest, if not the shortest, experimentally observed N-N bond lengths. For comparison, the N≡N bond distances in N_2 and $HN_2^{+\cdot}$ are 1.0976(2) and 1.09277(9) Å, respectively.[58,59]

Fig. S3 depicts the packing diagram of $N_2F^+Sb_2F_{11}^-$. The N_2F^+ cation lies between the Sb-F-Sb bend of the $Sb_2F_{11}^-$ anion at an angle of 68.4° with respect to the mean plane containing the

F6-Sb1-F7-Sb2-F12 atoms. As in the case of $N_2F^+SbF_6^-$, no close contacts are found to and from the N_2F^+ cation.

The geometry of the $Sb_2F_{11}^-$ anion also deserves a special comment. The Sb-F-Sb bridge is bent with an angle of 145.2(2)° and coplanar with the terminal fluorines, F6 and F12, which are eclipsed. The equatorial fluorine atoms of each SbF_5 group are staggered with a twist angle of ~31° (Fig. 2). The large variation in the structures of $Sb_2F_{11}^-$ anions in different compounds is due to its ease of deformation by crystal packing effects.[60,61]

Synthesis and Properties of $N_2F^+Sn_2F_9^-$. The only room-temperature stable N_2F^+ salts, previously reported were those derived from AsF_5 and SbF_5, while BF_3 and PF_5 do not form stable N_2F^+ salts.[3,9] Since SnF_4, with a pF^- value of 9.8,[62,63] is a stronger Lewis acid than either BF_3 or PF_5 and can form stable $N_2F_3^+$ and NF_4^+ salts,[26,27] it was interesting to explore the interaction between SnF_4 and *cis*–N_2F_2. Because SnF_4 is a highly polymeric solid, the reactions were carried out in anhydrous HF solution. It was found that SnF_4 reacts with excess *cis*–N_2F_2 in a 2 : 1 mole ratio giving white solids with the empirical composition $N_2F^+Sn_2F_9^-$ (Eq. 11).

$$cis\text{–}N_2F_2 + 2\ SnF_4 \rightarrow N_2F^+Sn_2F_9^- \qquad (11)$$

The products were characterized by vibrational spectroscopy (Figure S4, Table 4). They showed the three characteristic N_2F^+ bands and bands of variable intensities in the regions characteristic for Sn(IV) fluoride anions[26-28] indicating the presence of polyanions of variable composition and structure. The N_2F^+ bands also showed some splittings of variable intensities indicative of the presence of more than one form of the counterion. A similar observation for the existence of polymeric tin fluoride anions of different composition has previously been made in our study of $N_5^+SnF_5^-$ where the "SnF_5^-" anion was shown[28] by multinuclear NMR spectroscopy to be present as a mixture of $Sn_2F_{10}^{2-}$ and $Sn_4F_{20}^{4-}$. The preferred formation of $Sn_2F_9^-$ can be explained by the

fact that monomeric SnF_4 is a weaker Lewis acid than its oligomers, in accord with our general finding that oligomeric Lewis acids are stronger acids than their monomers.[62,63] Therefore, $Sn_2F_9^-$ salts are more stable than SnF_5^- salts, which in turn are more stable than SnF_6^{2-} salts. This was also demonstrated by us by carrying out metathetical reactions between $N_2F^+SbF_6^-$ and either $CsSnF_5$, Cs_2SnF_6 or Na_2SnF_6 in HF solution, which gave no evidence for the formation of stable N_2FSnF_5 or $(N_2F)_2SnF_6$ salts, but produced only some $N_2F^+Sn_2F_9^-$.

Further experimental evidence for the instability of $N_2F^+SnF_5^-$ was obtained in one instance when a product with a composition closer to 1 : 1 was accidentally obtained from the reaction of excess *cis*–N_2F_2 with SnF_4 in HF solution, when the removal time of unreacted N_2F_2 was shortened and the spectra of the solid product were immediately recorded (Fig. 3). These vibrational spectra showed the presence of anion bands resembling more closely those previously observed[28] for SnF_5^- in $N_5^+SnF_5^-$ and a set of bands due to *cis*–N_2F_2 trapped within the solid (Fig. 3). Their frequencies are very close to those of free gaseous *cis*–N_2F_2,[29] however, the rotational P and R branches, characteristic for the free gas, are missing. This demonstrates that N_2FSnF_5 decomposes at room temperature to $N_2FSn_2F_9$ and *cis*–N_2F_2 (Eq. 12).

$$2\ N_2F^+SnF_5^- \rightarrow N_2F^+Sn_2F_9^- + \textit{cis}\text{–}N_2F_2 \qquad (12)$$

The $Sn_2F_9^-$ anion most likely does not have a monomeric structure. Because tin prefers a coordination number of 6 towards fluorine, a monomeric anion would require three fluorine bridges, that is, the sharing of a common face. Based on the similarity of the coordination chemistry of Sn(IV) and Ti(IV) and the failure, despite of intensive efforts, of Mazej and Goreshnik[64] to find the corresponding triply-bridged monomeric $Ti_2F_9^-$ anion, its existence in tin chemistry is equally unlikely. Depending on the counter ion, they only found either tetrameric, pseudo-tetrahedral $Ti_4F_{18}^{2-}$ or polymeric, infinite double chain $(Ti_2F_9^-)_n$ anions. Based on the

complexity of our observed vibrational spectra, the analogy with the titanium system and our previous findings for SnF_5^-, it is very likely that $Sn_2F_9^-$ is also present as an oligomer or polymer.

Computational Results. Since precise experimental measurements of some of the thermodynamic properties of N_2F_2 and its isomerization process are very difficult due to its high reactivity and the small differences in the values between the two isomers, high-level electronic structure calculations can provide better values than experiment. A previous molecular orbital study by Lee and coworkers showed[4] that the calculated values strongly depend on the level of correlation treatment and the basis set. It was, therefore, desirable to perform these calculations at the highest available level.

Our calculated CCSD(T)/aVTZ value (Table 3) for the $r_{N\equiv N}$ distance in N_2F^+ is larger by 0.021 Å as compared to the experimental gas phase structure[52] and $r_{N\text{-}F}$ is shorter than experiment by 0.010 Å. The calculated r_e of N_2 ($^1\Sigma_g^+$) is 1.104 Å at this level[65] compared to the experimental value[66] of 1.0977 Å, a discrepancy of 0.006 Å. The calculated CEPA-1/[8,4,2,1] values[52] of $r_{N\equiv N}$ = 1.1040 Å and $r_{N\text{-}F}$ = 1.2521 Å for N_2F^+ are in somewhat better agreement with experiment than the CCSD(T)/aVTZ values. The anharmonic vibrational frequencies of N_2F^+, reported[9] previously as well as in the current work, are in excellent agreement with the calculated CCSD(T)/aVTZ harmonic frequencies (Table 4). The largest discrepancy was found for the F–N=N bend (π mode), which was calculated to be 20 cm^{-1} higher than the experimental value. Our calculated harmonic frequencies are also within about 20 cm^{-1} of the anharmonic CEPA-1 values.[52]

The experimental geometries of *cis*– and *trans*–N_2F_2 have been reported from electron diffraction (*cis* and *trans*)[67] and microwave spectroscopy (*cis*)[68] studies. Our CCSD(T)/aVTZ values for *cis*–N_2F_2 are in good agreement with the microwave structure[68] with the calculated

$r_{N\equiv N}$ and r_{N-F} distances being 0.011 Å and 0.003 Å, respectively, longer than the experimental values (Table 5). Our CCSD(T)/aVTZ values for *cis*– and *trans*–N_2F_2 are also in good agreement with the electron diffraction structures,[67] with the predicted r_{N-F} distances of both isomers being shorter than the experimental values. Comparison of the microwave and electron diffraction structures suggests that the electron diffraction r_{N-F} distances are too long. The calculations do reproduce the electron diffraction difference for the N-N bond lengths in the two isomers but not the difference in the N-F bond lengths. The substantial change in the ∠FNN for the c*is*- and *trans*-isomers of about 10° is reproduced by the calculations. The anharmonic vibrational frequencies of *cis*–N_2F_2 and *trans*–N_2F_2 have also been reported,[69,70] and agree well with our calculated CCSD(T)/aVTZ harmonic frequencies, with the largest discrepancy of 32 cm^{-1} found for the highest frequency a_1 mode of *cis*-N_2F_2 (Table 6).

The calculated heats of formation are given in Table 7. The components for the atomization energies are given in the Supporting Information. We predict *cis*-N_2F_2 to be more stable than *trans*-N_2F_2 by 1.4 kcal/mol at 298 K, consistent with other calculated values[4] and the experimental equilibrium measurements of Pankratov and Sokolov who found that within experimental error this value was close to zero.[48] We note that the current calculations are the most reliable values reported so far. Our calculated heat of formation of the less stable *trans*–N_2F_2 is within 0.1 kcal/mol of the reported experimental value.[43] However, our calculated value for *cis*–N_2F_2 is 1.7 kcal/mol higher than the reported experimental value,[47] due to the smaller calculated energy of isomerization.

In contrast to the small energy difference between the *cis*- and the *trans*-isomers which also represents the heat of isomerization, the activation energy barriers for the uncatalyzed isomerization of the free molecule are very high involving transition states which, depending on

the isomerization mechanism and the level and basis set used for the calculation, are at least 60 kcal/mol above the ground state. Two different mechanisms can be envisioned for the uncatalyzed *trans-cis* isomerization.

The first mechanism involves rotation about the N=N double bond resulting in a transition state of C_2 symmetry.

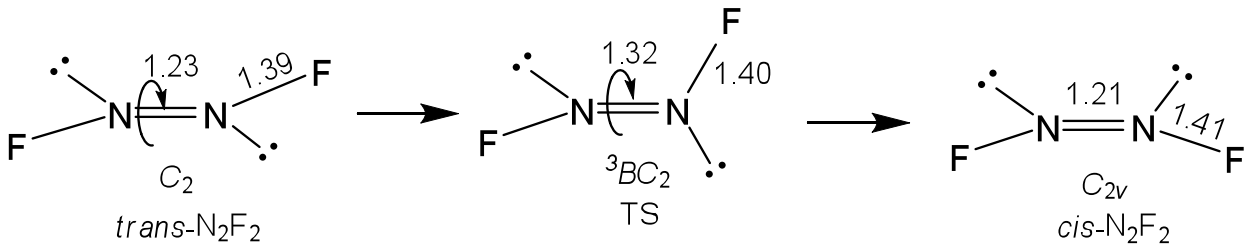

The calculated $^3B\ C_2$ minimum energy structure with a dihedral F-N-N-F angle of 89.8 ° (Table 6) lies 59.6 kcal/mol above the *cis*-isomer at 0 K. This represents the lower limit to the isomerization barrier on the singlet surface. The value of ~60 kcal/mol for rotation about the N=N bond is consistent with the value expected for the C=C π-bond.[71]

The second mechanism involves the in-plane inversion of one fluorine ligand with a transition state of C_s symmetry.

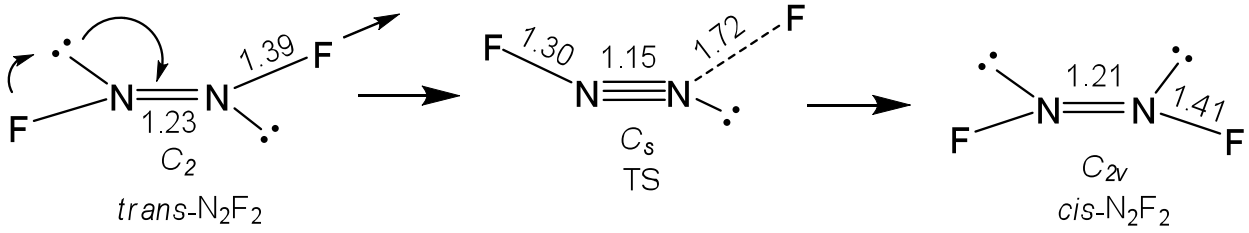

It has a structure similar to that of the N_2F^+ cation with a significantly shortened N-F bond of 1.30 Å, a very short N-N bond of 1.15 Å, and an F-N-N angle of 170 °. The second N-F bond is elongated to 1.72 Å. This transition state has an imaginary frequency of 883i cm^{-1} and lies 68.7 kcal/mol above the ground state. Thus, contrary to our previous speculation,[9] the

mechanism involving rotation about the N-N bond is energetically favored over the in-plane rearrangement of fluorine ligands, just as in an olefin with a comparable double bond.

Our high-level calculations for the isomerization barriers of the free N_2F_2 molecule are not expected to be in error by more than 1 to 2 kcal/mol and provide convincing evidence that the barrier is at least 60 kcal/mol. This result is in contrast to the previous CISD and CCSD calculations[4] which are too high by up to 20 kcal/mol, and the shock tube measurements[7] which reported an experimental barrier of 32 kcal/mol for this process. This value is probably highly inaccurate,[8] considering the great technical difficulties involved in making such a measurement for thermally labile molecules, and should be disregarded. This type of error is consistent with those found in similar shock tube experiments. This explanation is supported by an analysis of the bond dissociation energies in N_2F_2. The N_2F radical is barely stable with respect to loss of an F atom, so N_2F_2 will lose the second F atom as soon as the first N-F bond is broken. The energy for the reaction *cis*–$N_2F_2 \rightarrow N_2 + 2F$ is only 18.2 kcal/mol at 0 K. Hence, it is possible that isomerization was also occurring by a dissociation/association process. An FN=NF double bond dissociation is highly unlikely because its energy, defined by the reaction $N_2F_2 \rightarrow 2NF$, is 93 kcal/mol at 0 K, using $\Delta H_f(NF) = 55.6$ kcal/mol.[72] This value is substantially higher than the C=C bond dissociation energy in C_2F_4, defined by the reaction $C_2F_4 \rightarrow 2\,^1CF_2$ which is 68 kcal/mol.[73] In view of the relatively low thermal stability of N_2F_2 and the high barriers for the uncatalyzed isomerizations, the uncatalyzed isomerizations of *trans*–N_2F_2 are of lesser practical interest.

The F^+ affinity of N_2 (calculated using the experimental value[47] of $\Delta H_{f,0K}(F^+) = 419.40$ kcal/mol) is 127 kcal/mol at 0 K and falls in the lower range of the Christe/Dixon oxidizer strength scale[74] with values that are bracketed by those of OF_2 (122 kcal/mol) and BrF_3O (131

kcal/mol). This confirms the experimental observations that N_2F^+ is a very powerful oxidative fluorinator.

Contrary to our previous conclusion that Lewis acids do not catalyze the isomerization,[9] the results from the present study prove that strong Lewis acids do indeed catalyze this process. The catalytic effect of the Lewis acids can be readily understood by the similarity of the C_s transition state structure of the uncatalyzed isomerization with that of the N_2F^+ cation. The interaction of *trans*–N_2F_2 with a strong Lewis acid is likely to stretch one N-F bond, while at the same time shortening the other N-F bond as well as the N-N bond and increasing their F-N-N angle. This interaction greatly reduces the energy required for reaching the C_s transition state. It is also easy to understand that increasing Lewis acidity strength[62,63] lowers the barrier and the required isomerization temperature. Therefore, both *cis*–N_2F_2 and *trans*–N_2F_2 can react with strong Lewis acids to give N_2F^+ salts. The only difference is that the *cis*–isomer is more reactive. This increased reactivity of the *cis*-isomer can be readily explained. In both N_2F_2 isomers, each nitrogen atom possesses a sterically active free valence electron pair. The transformation of N_2F_2 to N_2F^+, requires the conversion of the N=N double bond into a N≡N triple bond by an overlap of electrons from these two free valence electron pairs. Obviously, this overlap is greatly facilitated in *cis*-N_2F_2 where these free pairs are on the same side of the molecule.

Another characteristic of the N_2F_2 reaction chemistry is the exclusive formation of *cis*-N_2F_2 when N_2F^+ reacts with F^- (Eq. 4). Why does one not obtain the typical 9:1 mole ratio of *cis*-N_2F_2 : *trans*-N_2F_2, observed for the *trans*-*cis* isomerization reactions? This feature can be readily explained by the charge distribution in N_2F^+. The central N atom carries the formal positive charge and, therefore, F^- attacks exclusively the central N atom, generating an F_2NN intermediate which rearranges itself by an in-plane α-fluorine migration to *cis*-N_2F_2.

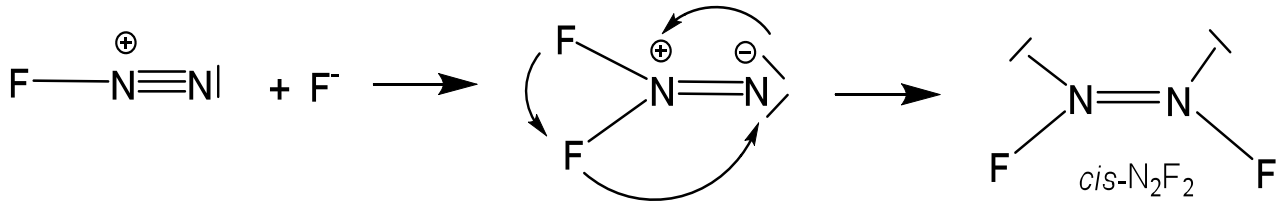

Because of the involvement of the $F_2N{=}N$ isomer in this reaction, it was interesting to explore this isomer in more detail. It lies 14.3 kcal/mol above the *cis*-isomer at 298 K, explaining its tendency to rearrange to the energetically favored *cis*-N_2F_2. Its calculated geometry and vibrational spectra are given in Tables 5 and 6, respectively. No experimental data are known for this isomer, and the spectrum originally attributed[75] to $F_2N{=}N$ by Sanborn is that of *cis*-N_2F_2.[3] Compared to *cis*-N_2F_2 and *trans*-N_2F_2, the calculated N-N bond length in $F_2N{=}N$ is dramatically shortened by about 0.10 Å, while the N-F bond lengths are increased by about 0.06 Å.

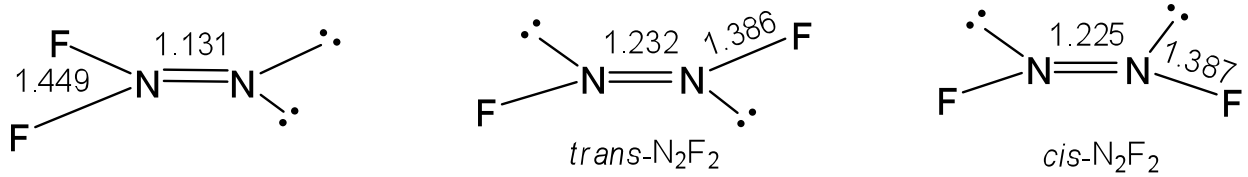

$\nu_{N\text{-}N}$ = 2059 cm^{-1} $\nu_{N\text{-}N}$ = 1550 cm^{-1} $\nu_{N\text{-}N}$ = 1557 cm^{-1}

Similarly, the N-N stretching frequency is increased by about 500 cm^{-1}, while the NF_2 stretching frequencies are decreased by an average of about 300 cm^{-1}, indicating that in $F_2N{=}N$, strong contributions from the following resonance structures must be invoked to describe its bonding appropriately.

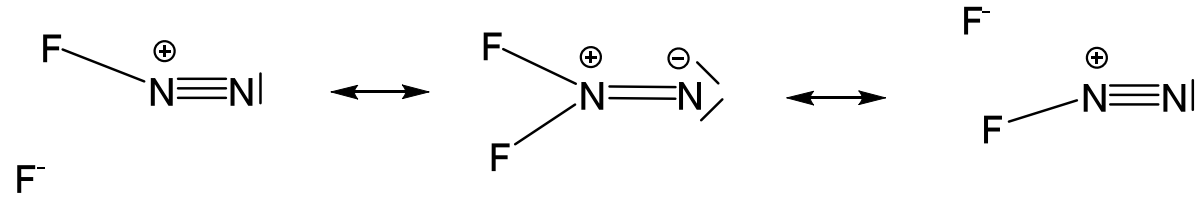

This strong contribution from highly polar N-F bonds resembles those encountered for F_3NO[10] and FNO.[11,12]

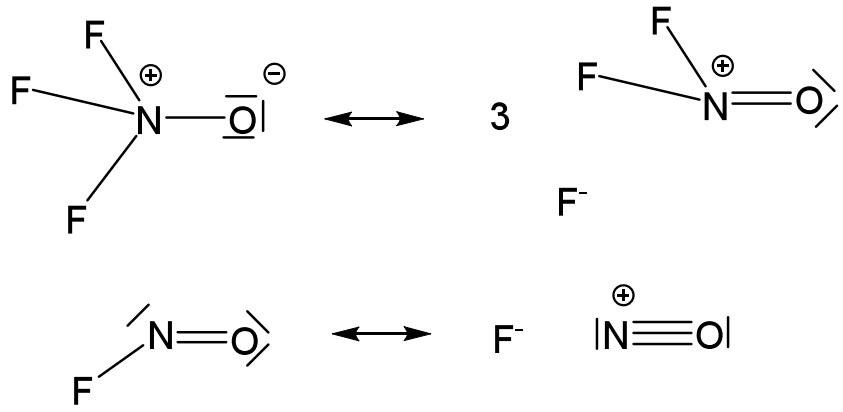

The driving forces behind these highly unusual resonance structures for nitrogen fluorides and oxofluorides is the desire of fluorine, which is more electronegative than oxygen or nitrogen, to carry the negative charges,

Conclusions

The present work describes improved methods for the synthesis of N_2F^+ salts, which are the key precursors to novel high energy density materials, such as N_5^+ salts. Important improvements include the use of cheap natural graphite flakes in place of expensive highly oriented pyrolytic graphite (HOPG) for the preparation of the first stage graphite-AsF_5 intercalate and of better catalysts for the N_2F_2 *trans–cis* isomerization, the elimination of extra reaction steps and significant reductions in the reaction times required for the synthesis of N_2F^+ salts, from several weeks to several days. Also, the first ordered crystal structure of an N_2F^+ salt was obtained, thus providing individual N≡N and N-F bond lengths for a direct comparison with the free molecule. These bonds are among the shortest experimentally observed N≡N and N-F bond lengths. Furthermore, the new N_2F^+ salt, $N_2F^+Sn_2F_9^-$, has been synthesized and characterized. High-level correlated molecular calculations were carried out and show that *cis*-N_2F_2 is more stable than *trans*-N_2F_2 by 1.4 kcal/mol at 298 K. In addition, the calculations demonstrate that

the lowest-energy uncatalyzed isomerization pathway involves rotation about the N=N double bond and has a barrier of 60 kcal/mol. This rotation barrier is substantially above the energy required for the dissociation of N_2F_2 to N_2 and 2F. Therefore, some of the N_2F_2 can dissociate before undergoing uncatalyzed isomerization resulting in autocatalysis by the decomposition products. It is shown that the *trans*-*cis* isomerization of N_2F_2 is catalyzed by strong Lewis acids, most likely involves a planar transition state of symmetry C_s, and yields a 9:1 equilibrium mixture of *cis*-N_2F_2 and *trans*-N_2F_2. Explanations are given for the increased reactivity of *cis*-N_2F_2 with Lewis acids and the exclusive formation of *cis*-N_2F_2 in the reaction of N_2F^+ with F^-. The geometry and vibrational frequencies of the $F_2N{=}N$ isomer have also been calculated and imply strong contributions from ionic N_2F^+ F^- resonance structures.

Acknowledgment. We gratefully acknowledge financial support of this work by the Air Force Office of Scientific Research, DARPA, the Office of Naval Research, the National Science Foundation, and the Department of Energy. DAD is indebted to the Robert Ramsay Endowment of the University of Alabama.

Supporting Information Available. Crystal data and structure refinement for $N_2F^+SbF_6^-$ (Table S1); atomic coordinates (x 10^4) and equivalent isotropic displacement parameters (Å^2 x 10^3) for $N_2F^+SbF_6^-$ (Table S2); bond lengths and angles for $N_2F^+SbF_6^-$ (Table S3); atomic coordinates (x 10^4) and equivalent isotropic displacement parameters (Å^2 x 10^3) for $N_2F^+Sb_2F_{11}^-$ (Table S4); CCSD(T)/aV*n*Z total energies (E_h) as a function of the basis set (Table S5); components for calculated atomization and reaction energies in kcal/mol (Table S6); ORTEP plot for $N_2F^+SbF_6^-$ with thermal ellipsoids at 30% probability level (Figure S1); packing diagram of $N_2F^+SbF_6^-$ along the *c*-axis (Figure S2); packing diagram of $N_2F^+Sb_2F_{11}^-$ along the *a*-axis (Figure S3); IR and Raman spectra of $N_2FSn_2F_9$ (Figure S4); and X-ray crystallographic file in CIF format for

the structure determinations of N_2FSbF_6 and $N_2FSb_2F_{11}$. This material is available free of charge via the internet at http://pubs.acs.org.

References

1. Christe, K. O.; Wilson, W. W.; Sheehy, J. A.; Boatz, J. A. *Angew. Chem. Intl. Ed*. **1999**, *38*, 2004.
2. Christe, K. O. *Propellants, Explosives, Pyrotechnics* **2007**, *32*, 194.
3. For an exhaustive review of the properties and chemistry of N_2F_2 see: *Gmelin Handbook of Inorganic Chemistry, Fluorine,* Springer Verlag; Berlin, 1986; Suppl. Vol. 4, pp 385-403.
4. Lee, T. J.; Rice, J. E.; Scuseria, G. E.; Schaefer, H. F., III *Theor. Chim. Acta* **1989**, *75*, 81.
5. Münch, V.; Selig, H. *J. Fluorine Chem.* **1980**, *15*, 235.
6. Colburn, C. B.; Johnson, F. A.; Kennedy, A.; McCallum, K.; Metzger, L. C.; Parker, C. O. *J. Am. Chem. Soc.* **1959,** *81*, 6397.
7. Binenboym, J.; Burcat, A.; Lifshitz, A.; Shamir, J. *J. Am. Chem. Soc.* **1966,** *88,* 5039.
8. Slanina, Z. *Chem. Phys. Lett.* **1977**, *50*, 418.
9. Christe, K. O.; Wilson, R. D.; Wilson, W. W.; Bau, R.; Sukumar, S.; Dixon, D. A. *J. Am. Chem. Soc*. **1991**, *113*, 3795.
10. Christe, K. O.; Curtis, E. C.; Schack, C. J. *Spectrochim. Acta* **1975,** *31A,* 1035.
11. Christe, K. O.; Guertin, J. P. *Inorg. Chem.* **1965,** *4*, 905.
12. Holleman-Wiberg, *Inorganic Chemistry,* Academic Press: San Diego, CA, **2001**, pg. 664.
13. Christe, K. O.; Wilson, W.W.; Schack, C. J. *J. Fluorine Chem.* **1978**, *11*, 71.
14. Christe, K. O.; Wilson, R. D.; Schack, C. J. *Inorg. Synth.* **1986,** *24,* 3.
15. SMART V 4.045 Software for the CCD Detector System, Bruker AXS, Madison, WI (1999).

16. SAINT V 4.035 Software for the CCD Detector System, Bruker AXS, Madison, WI (1999).

17. SADABS, Program for absorption correction for area detectors, Version 2.01, Bruker AXS, Madison, WI (2000).

18. Sheldrick, G. M. SHELXS-90, Program for the Solution of Crystal Structure, University of Göttingen, Germany, 1990.

19. Sheldrick, G. M. SHELXL-97, Program for the Refinement of Crystal Structure, University of Göttingen, Germany, 1997.

20. SHELXTL 5.10 for Windows NT, Program library for Structure Solution and Molecular Graphics, Bruker AXS, Madison, WI (1997).

21. Christe, K. O.; Wilson, R. D.; Sawodny, W. *J. Mol. Structure* **1971**, *8*, 245.

22. Ruff, J. K. *Inorg. Chem.* **1966**, *5*, 1971.

23. Shamir, J.; Binenboym, J. *J. Mol. Structure* **1969**, *4*, 100.

24. Moy, D.; Young, A. R. *J. Am. Chem. Soc.* **1965,** *87*, 1889.

25. Roesky, H. W.; Glemser, O.; Bormann, D. *Chem. Ber.* **1966,** *99*, 1589.

26. Christe, K. O.; Schack, C. J. *Inorg. Chem.* **1978,** *17*, 2749.

27. Christe, K. O.; Schack, C. J.; Wilson, R. D. *Inorg. Chem.* **1977,** *16*, 849.

28. Wilson, W. W.; Vij, A.; Vij, V.; Bernhardt, E.; Christe, K. O. *Chem. Eur. J.* **2003,** *9*, 2840.

29. King, S. T.; Overend, J. *Spectrochim. Acta* **1967,** *23A*, 61.

30. Feller, D.; Peterson, K. A.; Dixon, D. A. *J. Phys. Chem. A* WEB ASAP, Dec. 2009

31. Feller, D.; Peterson, K. A.; Dixon, D. A. *J. Chem. Phys.* **2008**, *129*, 204105.

32. Feller, D.; Dixon, D. A. *J. Phys. Chem. A* **2003**, *107*, 9641.

33. Purvis III, G. D.; Bartlett, R. J. *J. Chem. Phys.* **1982,** *76*, 1910.

34. Raghavachari, K.; Trucks, G. W.; Pople, J. A.; Head-Gordon, M. *Chem. Phys. Lett.* **1989**, *157*, 479.

35. Watts, J. D.; Gauss, J.; Bartlett, R. J. *J. Chem. Phys.* **1993**, *98*, 8718.

36. (a) Dunning, T. H., Jr. *J. Chem. Phys.* **1989**, *90*, 1007; (b) Kendall, R. A.; Dunning, T. H., Jr.; Harrison, R. J. *J. Chem. Phys.* **1992**, *96*, 6796; (c) Woon, D.E.; Dunning, T. H., Jr., *J. Chem. Phys.* **1993**, *98*, 1358; (d) Dunning, T. H., Jr.; Peterson, K. A.; Wilson, A. K. *J. Chem. Phys.* **2001**, *114*, 9244; (e) Wilson, A. K.; Woon, D. E.; Peterson, K. A.; Dunning, T. H., Jr., *J. Chem. Phys*. **1999**, *110*, 7667.

37. McQuarrie, D. A. *Statistical Mechanics*, University Science Books: Sausalito, CA, **2001.**

38. Curtiss, L. A.; Raghavachari, K.; Redfern, P. C.; Pople, J. A. *J. Chem. Phys.* **1997**, *106*, 1063.

39. MOLPRO a package of *ab initio* programs designed by Werner, H.-J.; and Knowles, P. J. version 2006, Universität Stuttgart, Stuttgart, Germany, University of Birmingham, Birmingham, United Kingdom, Amos, R. D.; Bernhardsson, A.; Berning, A.; Celani, P.; Cooper, D. L.; Deegan, M. J. O.; Dobbyn, A. J.; Eckert, F.; Hampel, C.; Hetzer, G.; Knowles, P. J.; Korona, T.; Lindh, R.; Lloyd, A. W.; McNicholas, S. J.; Manby, F. R.; Meyer, W.; Mura, M. E.; Nicklass, A.; Palmieri, P.; Pitzer, R.; Rauhut, G., Schütz, M.; Schumann, U.; Stoll, H., Stone, A. J.; Tarroni, R.; Thorsteinsson, T.; Werner, H.-J.

40. Rittby, M.; Bartlett, R. J. *J. Phys. Chem*. **1988**, *92*, 3033

41. Knowles, P. J.; Hampel, C.; Werner, H. –J. *J. Chem. Phys*. **1994**, *99*, 5219.

42. Deegan, M. J. O.; Knowles, P. J. *Chem. Phys. Lett*. **1994**, ***227,*** 321.

43. Peterson, K. A.; Woon, D. E.; Dunning, T. H., Jr. *J. Chem. Phys.* **1994**, *100*, 7410.

44. Peterson, K. A.; Dunning, T. H., Jr., *J. Chem. Phys.* **2002**, *117,* 10548.

45. C.E. Moore *"Atomic energy levels as derived from the analysis of optical spectra, Volume 1, H to V,"* U.S. National Bureau of Standards Circular 467, U.S. Department of Commerce, National Technical Information Service, COM-72-50282, Washington, D.C.; **1949.**

46. Davidson, E. R.; Ishikawa, Y;. Malli, G. L. *Chem. Phys. Lett.* **1981**, *84,* 226.

47. Chase, M. W., Jr.; NIST-JANAF Tables (4^{th} Edition), *J. Phys. Chem. Ref. Data*, Mono. 9, Suppl. 1 (1998).

48. Pankratov, A. V.; Sokolov, O. M. *Russ. J. Inorg. Chem.* **1966**, *11,* 943.

49. Christe, K. O.; Schack, C. J.; Wilson, R. D. *J. Fluorine Chem.* **1976**, *8,* 541.

50. Lustig, M. *Inorg. Chem.* **1965,** *4,* 104.

51. Pankratov, A. V.; Savenkova, N. I. *Zhur. Neorg. Khim.* **1968**, *13,* 2610.

52. Botschwina, P.; Sebald, P.; Bogey, M.; Demuynck, C.; Destombes, J. L. *J. Mol. Spectrosc.* **1992**, *153,* 255.

53. Mason, J.; Christe, K. O. *Inorg. Chem.* **1983,** *22, 1*849.

54. Glaser, R.; Choy, G. S. C. *J. Am. Chem. Soc.* **1993,** *115,* 2340.

55. Cacace, F.; Grandinetti, F.; Pepi, F. *Inorg. Chem.* **1995**, *34,* 1325.

56. Pulay, P.; Ruoff, A.; Sawodny, W. *Mol. Phys.* **1975**, 30, 1123.

57. Peters, N. J. S. *Chem. Phys. Lett.* **1987**, *142,* 76.

58. Owrutsky, J. C.; Gudeman, C. S.; Martner, C. C.; Tack, L. M.; Rosenbaum, N. H.; Saykally, R. J. *J. Chem. Phys.* **1986**, *84,* 605.

59. Huber, K. P.; Herzberg, G. *Constants of Diatomic Molecules*; Van Nostrand Reinhold: New York, 1979.

60. Willner, H.; Bodenbinder, M.; Broechler, R.; Hwang, G.; Rettig, S. J.; Trotter, J.; von Ahsen, B.; Westphal, U.; Jonas, V.; Thiel, W.; Aubke, F. *J. Am. Chem. Soc.* **2001,** *123*, 588.

61. Vij, A.; Wilson, W. W.; Vij, V.; Tham, F. S.; Sheehy, J. A.; Christe, K. O. *J. Am. Chem. Soc.* **2001,** *123*, 6308.

62. Christe, K. O.; Dixon, D. A.; McLemore, D.; Wilson, W. W.; Sheehy, J. A.; Boatz, J. A. *J. Fluorine Chem*. **2000**, *101*, 151.

63. Christe,K. O.; Dixon, D. A. *Paper 577, IN 3, presented at the 92nd Canadian Chemistry Conference,* May 30, 2009, Hamilton, ONT, Canada.

64. Mazej, G.; Goreshnik, E. *Inorg. Chem*. **2009**, *48*, 6918.

65. Matus, M. H.; Arduengo, III, A. J.; Dixon, D. A. *J. Phys. Chem. A* **2006**, *110*, 10116.

66. Huber, K. P.; Herzberg, G. Constants of Diatomic Molecules. Molecular Spectra and Molecular Structure, Vol. IV, Van Nostrand, Princeton, **1979**.

67. Bohn, R. K.; Bauer, S. H. *Inorg. Chem.* **1967**, *6*, 309.

68. Kuczkowski, R. L.; Wilson, E. B.; Jr. *J. Chem. Phys.* **1963**, *39*, 1030.

69. Shimanouchi, T., *J. Phys. Chem. Ref. Data* **1977**, 6, 993.

70. King, S. T.; Overend, J. *Spectrochim. Acta* **1966,** *22A*, 689.

71. M. T. Nguyen, M. H. Matus, W. A. Lester, Jr., and D. A. Dixon, *J. Phys. Chem. A* **2008**, *112*, 2082.

72. Feller, D.; Peterson, K. A.; Dixon, D. A. *J. Chem. Phys*. **2008**, *129*, 204015.

73. Dixon, D. A.; Feller, D.; Sandrone, G. *J. Phys. Chem. A* **1999**, *103*, 4744.

74. Christe, K. O.; Dixon, D. A. *J. Am. Chem. Soc.* **1992**, *114*, 2978.

75. Sanborn, R. H. *J. Chem. Phys*. **1960**, *33*, 1855.

Table 1. Crystal data and structure refinement for $N_2F^+Sb_2F_{11}^-$.

Chemical formula		F12 N2 Sb2
Formula weight		499.52
Temperature (°C)		-35 (2)
Space group		$P2_1/n$
Unit cell dimensions	*a* (Å)	7.558(2)
	b (Å)	9.926(2)
	c (Å)	14.103(2)
	β (°)	99.59(1)
Volume ($Å^3$)		1043.2(4)
Z		4
D_{calc} (g/cm^3)		3.181
Absorption coefficient (cm^{-1})		0.5329
Final R indices [I>2sigma(I)]		*R*1 = 0.0376
		*wR*2 = 0.0895
R indices (all data)		*R*1 = 0.0388
		*wR*2= 0.0903

Table 2. Bond lengths and angles for $N_2F^+Sb_2F_{11}^-$.

Bond Lengths (Å)

Sb(1)-F(3)	1.868(4)	Sb(2)-F(8)	1.876(4)
Sb(1)-F(2)	1.873(4)	Sb(2)-F(11)	1.883(4)
Sb(1)-F(6)	1.879(4)	Sb(2)-F(10)	1.885(4)
Sb(1)-F(5)	1.887(4)	Sb(2)-F(12)	1.901(4)
Sb(1)-F(4)	1.894(4)	Sb(2)-F(7)	2.076(4)
Sb(1)-F(7)	2.077(4)	F(1)-N(1)	1.257(8)
Sb(2)-F(9)	1.865(4)	N(1)-N(2)	1.089(9)

Bond Angles (°)

N(2)-N(1)-F(1)	179.2(7)	F(8)-Sb(2)-F(7)-Sb(1)	114.5(4)
F(3)-Sb(1)-F(2)	89.6(2)	F(9)-Sb(2)-F(7)	85.64(18)
F(3)-Sb(1)-F(6)	95.9(2)	Sb(2)-F(7)-Sb(1)	145.2(2)
F(2)-Sb(1)-F(6)	95.2(2)	F(8)-Sb(2)-F(7)	86.46(18)
F(3)-Sb(1)-F(5)	172.1(2)	F(11)-Sb(2)-F(7)	84.74(17)
F(2)-Sb(1)-F(5)	89.8(2)	F(10)-Sb(2)-F(7)	86.6(2)
F(6)-Sb(1)-F(5)	92.0(2)	F(12)-Sb(2)-F(7)	178.61(18)
F(3)-Sb(1)-F(4)	90.8(2)	F(9)-Sb(2)-F(8)	90.5(2)
F(2)-Sb(1)-F(4)	170.3(2)	F(9)-Sb(2)-F(11)	170.39(19)
F(6)-Sb(1)-F(4)	94.4(2)	F(8)-Sb(2)-F(11)	89.0(2)
F(5)-Sb(1)-F(4)	88.5(2)	F(9)-Sb(2)-F(10)	90.4(2)
F(3)-Sb(1)-F(7)	87.56(18)	F(8)-Sb(2)-F(10)	172.9(2)
F(2)-Sb(1)-F(7)	87.55(19)	F(11)-Sb(2)-F(10)	88.9(2)
F(6)-Sb(1)-F(7)	175.64(17)	F(9)-Sb(2)-F(12)	95.7(2)
F(5)-Sb(1)-F(7)	84.56(18)	F(8)-Sb(2)-F(12)	93.5(2)
F(4)-Sb(1)-F(7)	82.80(17)	F(11)-Sb(2)-F(12)	93.86(19)
		F(10)-Sb(2)-F(12)	93.4(2)

Torsion Angles (°)

F(9)-Sb(2)-F(7)-Sb(1)	-154.8(4)

F(11)-Sb(2)-F(7)-Sb(1)	25.1(4)	F(10)-Sb(2)-F(7)-Sb(1)	-64.1(4)
F(6)-Sb(1)-F(7)-Sb(2)	-19(3)	F(12)-Sb(2)-F(7)-Sb(1)	26(8)
F(5)-Sb(1)-F(7)-Sb(2)	-56.9(4)	F(3)-Sb(1)-F(7)-Sb(2)	123.3(4)
F(4)-Sb(1)-F(7)-Sb(2)	32.2(4)	F(2)-Sb(1)-F(7)-Sb(2)	-147.0(4)

Table 3. Calculated and experimental bond distances (Å) for N_2F^+.

Molecule	**Method**	$r_{N\equiv N}$	r_{N-F}	$\Sigma(r_{N\equiv N} + r_{N-F})$
$N_2F^+AsF_6^-$	x-ray[9]	(1.099)[a]	(1.217)[a]	2.316 (12)
$N_2F^+SbF_6^-$	x-ray[9]	(1.110)[a]	(1.230)[a]	2.340 (9)
$N_2F^+Sb_2F_{11}^-$	x-ray(this work)	1.089 (9)	1.257 (8)	2.346 (9)
N_2F^+(gas)	Millimeter spectroscopy[49]	1.1034	1.2461	2.3495
N_2F^+(gas)	CCSD(T)/aVTZ	1.1246	1.2357	2.360
N_2F^+(gas)	CEPA-1/[8,4,2,1] [49]	1.1040	1.2521	2.3561

[a] Obtained by partitioning the experimentally observed sum in the same ratio as that calculated at the LDFS2 level.